SKYRME-RPA DESCRIPTION OF SPIN-FLIP M1 GIANT RESONANCE

P. Vesely[1], J. Kvasil[1], V.O. Nesterenko[2], W. Kleinig[2,3], P.-G. Reinhard[4], and V.Yu. Ponomarev [5]
[1] *Institute of Particle and Nuclear Physics, Charles University, CZ-18000, Praha 8, Czech Republic*
[2] *Laboratory of Theoretical Physics, Joint Institute for Nuclear Research, Dubna, Moscow region, 141980, Russia*
[3] *Technische Universität Dresden, Inst. für Analysis,D-01062, Dresden, Germany*
[4] *Institut für Theoretische Physik II, Universität Erlangen, D-91058, Erlangen, Germany and*
[5] *Institut für Kernphysik, Technische Universität Darmstadt, D-64289 Darmstadt, Germany*
(Dated: July 8, 2009)

The spin-flip M1 giant resonance is explored in the framework of Random Phase Approximation on the basis of the Skyrme energy functional. A representative set of eight Skyrme parameterizations (SkT6, SkM*, SLy6, SG2, SkO, SkO', SkI4, and SV-bas) is used. Light and heavy, spherical and deformed nuclei (^{48}Ca, ^{158}Gd, ^{208}Pb, and ^{238}U) are considered. The calculations show that spin densities play a crucial role in forming the collective shift in the spectrum. The interplay of the collective shift and spin-orbit splitting determines the quality of the description. None of the considered Skyrme parameterizations is able to describe simultaneously the M1 strength distribution in closed-shell and open-shell nuclei. It is found that the problem lies in the relative positions of proton and neutron spin-orbit splitting. Necessity to involve the tensor and isovector spin-orbit interaction is called for.

I. INTRODUCTION

Nuclear density-functional-theory (DFT), with the most prominent representatives being Skyrme-Hartree-Fock (SHF), the Gogny forces, and the relativistic mean-field model, achieved a high level of quality in the description of ground state and dynamics of atomic nuclei [1, 2, 3]. Most applications for nuclear dynamics up to now have been concerned with electrical excitation modes (natural parity). The description works generally well, except for some persistent problems with the isovector giant resonance (GR) in light nuclei [4, 5]. Much less work has been done yet for magnetic excitations (unnatural parity). At the same time, magnetic modes are sensitive to a different class of force parameters, namely those related to spin. An exploration of magnetic resonances, like spin-flip M1, could essentially improve the spin-orbit interaction. Magnetic modes could clarify the role of still vague tensor interaction [6]. Also, the spin-flip M1 resonance is a counterpart of the spin-isospin Gamow-Teller resonance which is of great current interest in connection with astrophysical problems [2, 3, 7, 8, 9]. Investigation of the M1 resonance could be useful in this connection as well.

There are many studies of the spin-flip M1 mode within simple models beyond the DFT, see e.g. reviews [10, 11, 12]. At the same time, as far as we know, a DFT treatment is limited to a few publications using SHF [13, 14] and even that is not carried through fully consistently. The work [13] uses a hybrid model with partial inclusion of SHF in the Landau-Migdal formulation [13]. The other study [14] uses the early Skyrme forces and omits the crucial spin density. These studies, being a useful first step, are not satisfactory for nowadays demands.

The present study aims at a fully self-consistent description of the spin-flip M1 mode in the framework of SHF. Previous investigations for Gamow-Teller [7, 8, 9] and spin-flip M1 modes [13] hint that spin-density response could be decisive to get a sizeable collective shift. So all the Skyrme terms with spin density (usually omitted in calculations for electric modes) have to be implemented and scrutinized. Furthermore, because of the obvious importance of spin-orbit splitting, the responses delivered by spin-orbit and tensor interactions have to be inspected as well. Since the quality of the description may depend on the particular Skyrme parameterization as well as on nuclear shape and mass region, a variety of parameterizations should be checked for light and heavy, spherical and deformed nuclei. Note that the M1 mode in heavy open-shell nuclei (rare-earth and actinides) exhibits a pronounced double-peak structure [15, 16] while closed-shell nuclei (^{48}Ca, ^{208}Pb, ...) show only one peak [17, 18, 19]. All these demands are met in the present study which, to the best of our knowledge, is the first systematic and self-consistent SHF exploration of spin-flip M1.

II. DETAILS OF CALCULATIONS

We will consider the resonance in the doubly-magic nuclei ^{48}Ca and ^{208}Pb and axially deformed nuclei ^{158}Gd and ^{238}U. A representative set of eight SHF parameterizations is used: SkT6 [20], SkO [21], SkO' [21], SG2 [22], SkM* [23], SLy6 [24], SkI4 [25], and SV-bas [5]. They exhibit a variety of effective masses (from m^*/m=1 in SkT6 down to 0.65 in SkI4) and other nuclear matter characteristics. Some of the forces (SLy6) were found favorable in the description of E1(T=1) GR [26, 27, 28, 29]. Others were used in studies of Gamow-Teller strength (SG2, SkO') [7, 8, 9, 22] or peculiarities of spin-orbit splitting (SkI4) [25]. The forces SkT6, SG2 and SkO' involve the tensor spin-orbit term. The parameterization SV-bas represents one of the latest upgrades in SHF.

The calculations are performed within the self-consistent separable random-phase-approximation

(SRPA) approach based on factorized Skyrme residual interaction [26, 30, 31]. The self-consistent factorization considerably reduces the computational expense of RPA while maintaining a high accuracy. This allows to perform systematic studies in both spherical and deformed (heavy and super-heavy) nuclei [26, 27, 28, 29, 30]. The residual interaction includes all contributions arising from the SHF functional as well as the Coulomb (direct and exchange) and pairing (at BCS level) terms [26, 31]).

The Skyrme energy density to be exploited reads [1, 3]

$$\begin{aligned}
\mathcal{H}_{\rm Sk} \;=\; & \frac{b_0}{2}\rho^2 - \frac{b'_0}{2}\sum_q \rho_q^2 + \frac{b_3}{3}\rho^{\alpha+2} - \frac{b'_3}{3}\rho^\alpha \sum_q \rho_q^2 \\
& + b_1(\rho\tau - \mathbf{j}^2) - b'_1 \sum_q (\rho_q\tau_q - \mathbf{j}_q^2) \\
& - \frac{b_2}{2}\rho\Delta\rho + \frac{b'_2}{2}\sum_q \rho_q\Delta\rho_q \\
& - b_4(\rho\nabla\mathbf{J} + (\nabla\times\mathbf{j})\cdot\mathbf{s}) \\
& - b'_4 \sum_q (\rho_q\nabla\mathbf{J}_q + (\nabla\times\mathbf{j}_q)\cdot\mathbf{s}_q) \\
& + \frac{\tilde{b}_0}{2}\mathbf{s}^2 - \frac{\tilde{b}'_0}{2}\sum_q \mathbf{s}_q^2 + \frac{\tilde{b}_3}{3}\rho^\alpha\mathbf{s}^2 - \frac{\tilde{b}'_3}{3}\rho^\alpha\sum_q \mathbf{s}_q^2 \\
& - \frac{\tilde{b}_2}{2}\mathbf{s}\cdot\Delta\mathbf{s} + \frac{\tilde{b}'_2}{2}\sum_q \mathbf{s}_q\cdot\Delta\mathbf{s}_q \\
& + \gamma_{\rm T}\tilde{b}_1(\mathbf{s}\cdot\mathbf{T} - \mathbf{J}^2) + \gamma_{\rm T}\tilde{b}'_1\sum_q(\mathbf{s}_q\cdot\mathbf{T}_q - \mathbf{J}_q^2) \qquad (1)
\end{aligned}$$

where b_i, b'_i, $\tilde{b}_i$, $\tilde{b}'_i$ are the force parameters. This functional involves time-even (nucleon ρ_q, kinetic-energy τ_q, spin-orbit $\mathbf{J}_q$) and time-odd (current $\mathbf{j}_q$, spin $\mathbf{s}_q$, vector kinetic-energy $\mathbf{T}_q$) densities where q denotes protons and neutrons. Densities without index, like $\rho = \rho_p + \rho_n$, denote total densities. The contributions with b_i (i=0,1,2,3,4) and b'_i (i=0,1,2,3) are the standard terms responsible for ground state properties and electric excitations of even-even nuclei [1, 3]. In the standard SHF, the isovector spin-orbit interaction is linked to the isoscalar one by $b'_4 = b_4$. The tensor spin-orbit terms $\propto \tilde{b}_1, \tilde{b}'_1$ are often skipped. In (1) they can be switched by the parameter $\gamma_{\rm T}$. The spin terms with $\tilde{b}_i, \tilde{b}'_i$ become relevant only for odd nuclei and magnetic modes in even-even nuclei. Though $\tilde{b}_i, \tilde{b}'_i$ may be uniquely determined as functions of b_i, b'_i [3], their values were not yet well tested by nuclear data. Moreover, following a strict DFT, they can be considered as free parameters. Just these spin terms may be of a paramount importance for the spin-slip M1. Hence all them are taken into account in SRPA.

In addition to second functional derivatives entering the SRPA residual interaction for electric modes,

$$\frac{\delta^2 E}{\delta\rho_{q'}\delta\rho_q}\,,\frac{\delta^2 E}{\delta\tau_{q'}\delta\rho_q}\,,\frac{\delta^2 E}{\delta\mathbf{J}_{q'}\delta\rho_q}\,,\frac{\delta^2 E}{\delta\mathbf{j}_{q'}\delta\mathbf{j}_q}\,, \qquad (2)$$

the present treatment also involves the terms with

$$\frac{\delta^2 E}{\delta\mathbf{j}_{q'}\delta\mathbf{s}_q}\,,\frac{\delta^2 E}{\delta\mathbf{s}_{q'}\delta\mathbf{s}_q}\,,\frac{\delta^2 E}{\delta\mathbf{J}_{q'}\delta\mathbf{J}_q}\,,\frac{\delta^2 E}{\delta\mathbf{T}_{q'}\delta\mathbf{s}_q}\,. \qquad (3)$$

SRPA generators include spin and orbital input operators $\hat{P}^s_q = R(r)\hat{s}^q_+$ and $\hat{P}^l_q = R(r)\hat{l}^q_+$ with $R(r)$ being 1 or r^2. In deformed nuclei, to take into account the coupling between spin and quadrupole $K^\pi = 1^+$ states, the quadrupole generator $\hat{Q}_q = r^2 Y_{21}(\Theta)$ is also added. The convergence of the results with including more generators was checked. See details in [32].

The SHF calculations employ a coordinate-space grid with the mesh size 0.7 fm. For deformed nuclei, cylindrical coordinates are used and the equilibrium quadrupole deformation is found by minimization of the total energy [26, 29]. The single-particle spectrum involves all levels from the bottom of the mean field well up to +20 MeV. In the heaviest nucleus under consideration, ^{238}U, this results in ∼17000 two-quasiparticle (2qp) $K^\pi = 1^+$ pairs with the excitation energies up to 50-70 MeV. Note that for electric E1(T=1) and E2(T=0) excitations such single-particle space provides a satisfying exhaustion of the energy-weighted sum rules [28].

The spectral distribution of the spin-flip M1 mode with $K^\pi = 1^+$ is presented as the strength function

$$S(M1;\omega) = \sum_{\nu\neq 0} |\langle\Psi_\nu|\hat{M}|\Psi_0\rangle|^2 \zeta(\omega-\omega_\nu) \qquad (4)$$

where $\zeta(\omega-\omega_\nu) = \Delta/[2\pi[(\omega-\omega_\nu)^2 + \frac{\Delta^2}{4}]]$ is a Lorentz weight with the averaging parameter Δ=1 MeV. Such averaging width is found optimal for the comparison with experiment and simulation of broadening effects beyond SRPA (escape widths, coupling with complex configurations). Further, Ψ_0 is the ground state, ν runs over the RPA $K^\pi = 1^+$ states with energies ω_ν and wave functions Ψ_ν. The operator of spin-flip M1 transition reads in standard notation as $\hat{M} = \mu_B\sqrt{\frac{3}{8\pi}}\sum_q[g^q_s\hat{s}^q_+ + g^q_l\hat{l}^q_+]$ with spin g-factors $g^p_s = 5.58\varsigma_p$ and $g^n_s = -3.82\varsigma_n$ quenched by ς_p=0.68 and ς_n=0.64. As we are interested in the spin-flip M1, the orbital response is omitted, i.e. we put $g^q_l = 0$. Note that in the experimental data [15, 16, 17, 18, 19] used for the comparison, the orbital contribution is strongly suppressed. The strength function (4) is computed directly, i.e. without calculation of RPA states ν, which additionally reduces the computation effort [26, 30, 31, 32].

More details of SRPA formalism are given in the appendices A, B, and C.

III. RESULTS AND DISCUSSION

In Fig. 1 the collective shifts of the main resonance peak in ^{48}Ca, ^{208}Pb, ^{158}Gd, and ^{238}U, obtained with different Skyrme parameterizations, are shown. The shifts

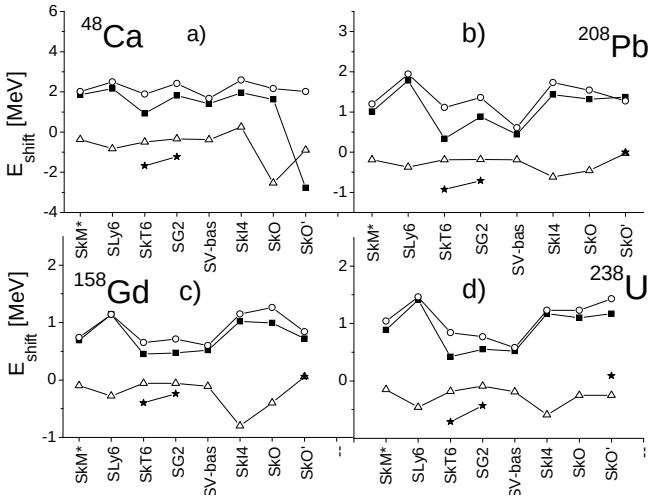

FIG. 1: Collective shifts of the M1 peak for different Skyrme parameterizations (as indicated along the x-axis) in ^{48}Ca, ^{208}Pb, ^{158}Gd and ^{238}U. The plots exhibit the total (black boxes) shifts as well as the partial ones with $\tilde{b}_0$ and $\tilde{b}_3$ (open circles), $\tilde{b}_2$ (open triangles), and $\tilde{b}_1$ (stars). The $\tilde{b}_1$ contribution exists only for SkT6, SG2, and SkO'. For better view the symbols are connected by lines.

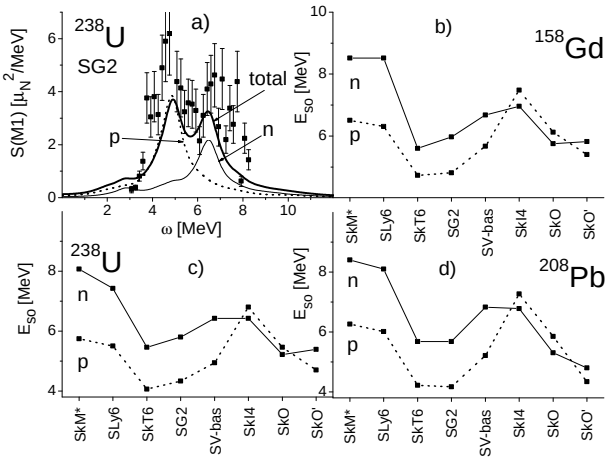

FIG. 2: a): The spin-flip M1 resonance in ^{238}U calculated with SG2 force: total (bold solid line), proton (dotted line) and neutron (solid line) strengths. The experimental data [15] are given by black boxes with bars. b)-d): proton and neutron unperturbed spin-orbit splittings for different Skyrme force in ^{158}Gd, ^{238}U, and ^{208}Pb.

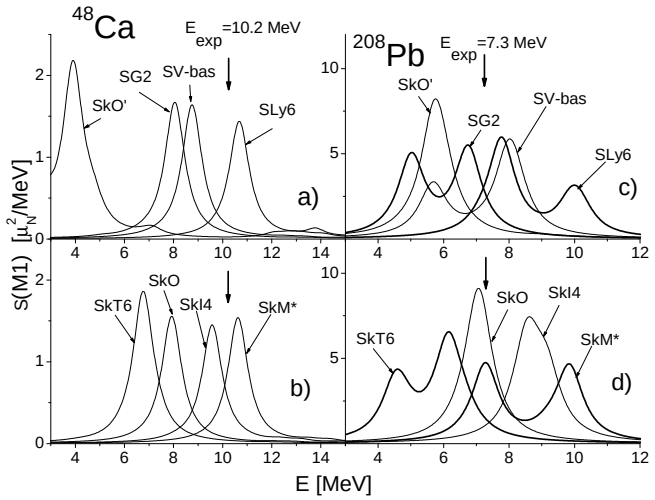

FIG. 3: The spin-flip M1 resonance in ^{48}Ca (left) and ^{208}Pb (right) calculated within SRPA for 8 Skyrme forces as indicated. For better distinguishability, the strength in ^{208}Pb for SG2, SLy6, SkT6 and SkM* is depicted by the bold line. The experimental energies in ^{48}Ca [17] and ^{208}Pb [18] are marked by vertical arrows.

are defined as $E_{shift} = E_{SRPA} - E_{2qp}$, i.e. as a difference in the energies of SRPA and unperturbed two-quasiparticle M1 peaks. The 2qp strength is calculated by using (4) without the residual interaction. In addition to the total shift, the contributions from different spin-density dependent terms as well as from the tensor force (for SkT6, SG2 and SkO') are shown. It is seen that the total collective shifts are generally modest and vary from 1-2 MeV in ^{48}Ca to 0.5-2 MeV in ^{208}Pb and 0.5-1.5 MeV in ^{158}Gd and ^{238}U. The low value emerges from contributions pulling in different directions. This holds for the separate shifts from $\tilde{b}_0$ and $\tilde{b}_3$ (not disentangled here). The $\tilde{b}_2$-term gives a negative shift in contrast to the positive one from $\tilde{b}_0, \tilde{b}_3$. Anyway the contribution from $\tilde{b}_0, \tilde{b}_3$ usually dominates thus giving the total upshift in accordance with isovector character of the resonance. All the forces give generally similar results. Note a sizable contribution of the tensor interaction for SkT6 and SG2. For SkO' this contribution is negligible, except for ^{48}Ca where it is so strong that gives a negative total E_{shift}. It should be emphasized that the non-spin contributions (with b_i, b'_i) alone do not provide any collective shift and leave the M1 strength unperturbed. The whole shift is produced by the spin-dependent terms $\propto \tilde{b}_i, \tilde{b}'_i$.

The calculations give a reasonable summed B(M1) strength. In the interval 0-45 MeV the unperturbed strength is 3.2 and 18.4-18.6 μ_N^2 in ^{48}Ca and ^{208}Pb. The residual interaction changes these values and we have 2.5 - 4.8 μ_N^2 in ^{48}Ca and 14.8 - 17.3 μ_N^2 in ^{208}Pb as compared with experimental values ~ 5.3 μ_N^2 [17] and ~ 17.9 μ_N^2 [18], respectively. Note a strong collective effect in ^{48}Ca.

It is well known that proton and neutron spin-orbit splittings E_{so}^q represent another crucial ingredient in description of spin-flip M1 mode [10, 11, 12]. Usually $E_{so}^p < E_{so}^n$ which leads in rare-earth and actinide nuclei to a two-peak structure of the resonance with dominant proton (neutron) origin of the lower (upper) peak. This is demonstrated for ^{238}U in Fig. 2a) where the proton and neutron components of the M1 mode, obtained with ς_p=0.68, ς_n=0 and ς_p=0, ς_n=0.64, respectively, are shown. Panels b)-d) exhibit proton and neutron splittings E_{so}^q for different Skyrme forces. The splittings are evaluated from centroids of the proton and neutron peaks

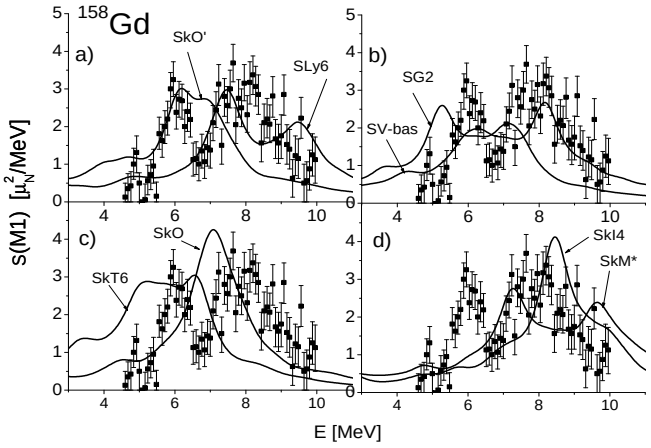

FIG. 4: The spin-flip M1 resonance in ^{158}Gd described with eight Skyrme parameterizations as indicated. The experimental data are from [15, 16].

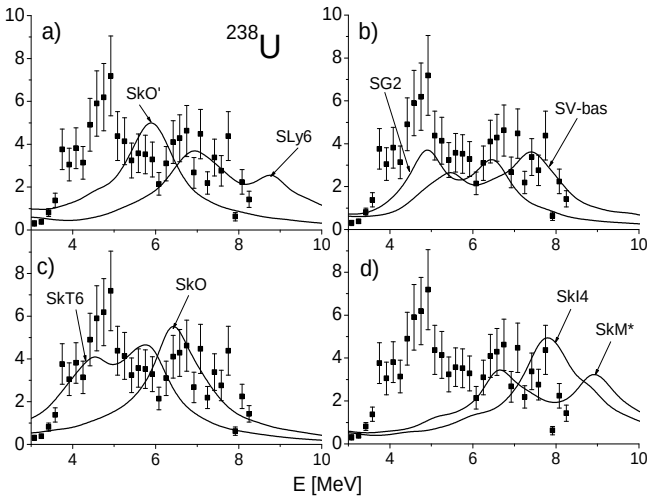

FIG. 5: The same as in Fig. 4 for ^{238}U.

of the unperturbed M1 strength. The results strongly depend on the parameterization. In most of the cases we have $E^p_{so} < E^n_{so}$ with $E^{np}_{so} = |E^p_{so} - E^n_{so}|$ ∼1-2 MeV but SkI4, SkO and SkO' give very close splittings with even $E^p_{so} > E^n_{so}$ for SkI4 and SkO. The latter is related with a low value of b_4 and nonzero value of b'_4 in SkI4. Note that the experimental proton-neutron splitting in M1 gross structure is ∼ 2 MeV in ^{158}Gd and ^{238}U [15, 16] and zero in ^{208}Pb [18, 19].

In Fig. 3 the SRPA M1 strength function (4) in spherical doubly-magic nuclei ^{48}Ca and ^{208}Pb is presented. In ^{48}Ca, the resonance is produced only by neutron spin-flip transition $\nu(1f^{-1}_{7/2}, 1f_{5/2})$ yielding the one-peak structure. This feature is correctly reproduced by all the parameterizations. However, most of them underestimate the resonance energy (with worst SkO' case because of the strong and possibly wrong tensor contribution) and only the forces SLy6, SkI4, and SkM* (with maximal E^n_{so}) give the M1 energy close to experiment. The success of these forces is obviously determined by a suitable neutron spin-orbit splitting.

However, the same figure shows that in ^{208}Pb the forces SLy6, SkI4, and SkM* considerably overestimate the M1 energy while the best result is achieved by SkO. Note that only SkO, SkO' and SkI4, all having a small E^{np}_{so}, give a one-peak resonance structure in accordance with experiment [18]. This is because only for these parameterizations the interaction energy (≈ collective shift) is larger than E^{np}_{so} and so a significant mixture of proton and neutron components with forming of a one-peak resonance becomes possible. The other forces have too large E^{np}_{so} and produce the two-peak structure. This demonstrates the great importance of the interplay between the residual interaction and relative proton and neutron spin-orbit splitting E^{np}_{so} for the description of spin-flip M1.

Figs. 4 and 5 present SRPA results for deformed ^{158}Gd and ^{238}U. Here, in contrast to ^{208}Pb, the experiment yields a double-peak structure and so the one-peak picture from SkO, SkO', and SkI4 fails. The description is generally quite poor, with exception of SV-bas in ^{158}Gd and SG2 in ^{238}U. Thus we see that any Skyrme parameterization fails to describe simultaneously the one-peak structure in closed-shell nuclei and two-peak structure in open-shell nuclei. The reason is yet unclear. However, the relative spin-orbit splitting E^{np}_{so} is evidently one of the key factor and it is important to find a way to control it.

Fig. 6 explores the influence of the spin-orbit contributions by systematic variation of tensor spin-orbit (panel a) and isovector spin-orbit terms (panel b). Variation of the tensor spin-orbit strength shifts significantly both E^n_{so} and E^p_{so} while leaving the relative order unchanged. But the variation of the isovector spin-orbit strength b'_4 has a strong effect on the relative positions. So by simultaneous monitoring tensor and isovector spin-orbit interactions one may control better the spin-orbit splittings. Besides the strong effect on single-particle energies, these interactions also affect the collective shifts (see Fig. 1). Altogether they represent very promising tool for further improvement of the description of spin-flip M1 modes.

IV. CONCLUSIONS

We have studied the ability of Skyrme forces to describe the spin-flip M1 resonance using RPA with self-consistent factorized residual interaction. The results show that the terms with spin and spin-orbit densities are responsible for a sizable collective shift of the resonance peak. The spin-orbit splitting of the underlying two-quasiparticle states is of crucial importance for the final pattern of the spectrum (single-peak versus double-

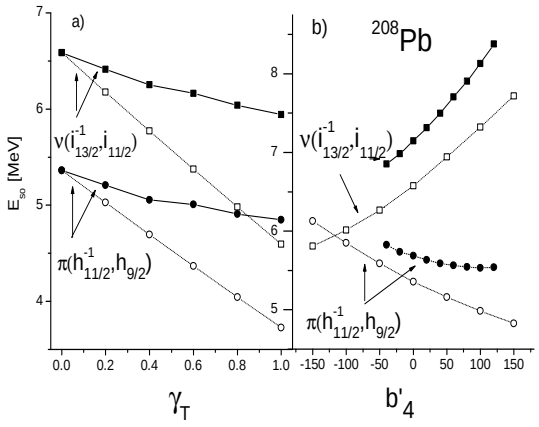

FIG. 6: Dependence of unperturbed spin-orbit splitting for proton $\pi(h_{11/2}^{-1}, h_{9/2})$ and neutron $\nu(i_{13/2}^{-1}, i_{11/2})$ configurations in ^{208}Pb on (a) the attenuation $0 \leq \gamma_T \leq 1$ for tensor interaction and (b) the parameter b'_4 of isovector spin-orbit interaction. Skyrme parameterizations with varied γ_T or b'_4 are used [5]. The proton (neutron) splittings are marked by circles (boxes). Filled symbols mark results for parameterizations refitted for given γ_T or b'_4. Open symbols stand for SV-bas where only γ_T or b'_4 are varied, i.e. without refitting.

peak structure). The residual interaction tends to mix of proton and neutron spin-orbit partners and so works towards a one-peak structure, as in ^{208}Pb. However, a large difference between neutron and proton spin-orbit splitting inhibits this mixing and produces two distinct proton and neutron peaks, as seen experimentally in rare-earth and actinide nuclei.

None of eight Skyrme parameterizations used in the present study is able to describe simultaneously the one-peak and two-peak structures in closed-shell and open-shell nuclei. In most of the cases, the resonance energies are badly reproduced as well. A first exploration indicates that fine-tuning of tensor and isovector spin-orbit interactions could improve the description, as they affect both the spin-orbit splittings and collective shifts. Work in this direction is in progress. A corresponding improvement of the Skyrme parameterizations would be important not only for description of spin-flip M1 resonance (which is a challenge itself) but also for better treatment of the spin-orbit interaction in nuclei.

Acknowledgments

The work was partly supported by the grants DFG-322/11-1, Heisenberg-Landau (Germany - BLTP JINR), and Votruba - Blokhintsev (Czech Republic - BLTP JINR). W.K. and P.-G.R. are grateful for the BMBF support under contracts 06 DD 139D and 06 ER 808. Being a part of the research plan MSM 0021620859 (Ministry of Education of the Czech Republic) this work was also funded by Czech grant agency (grant No. 202/06/0363). V.Yu.P. thanks the DFG contract SFB 634.

APPENDIX A: SRPA

The SRPA formalism is given elsewhere [26, 30, 31]. So here we will present only principle points and peculiarities pertinent to magnetic excitations. The SRPA approximates the residual interaction of Skyrme RPA in a factorized (separable) form as

$$\hat{V}_{\rm res}^{\rm sep} = -\frac{1}{2}\sum_{qq'}\sum_{k,k'=1}^{K}\{\kappa_{qk,q'k'}\hat{X}_{qk}\hat{X}_{q'k'} + \eta_{qk,q'k'}\hat{Y}_{qk}\hat{Y}_{q'k'}\} \tag{A1}$$

where the indices q and q' label neutrons and protons, k numbers the separable terms, $\hat{X}_{qk}$ and $\hat{Y}_{qk}$ are time-even and time-odd hermitian one-body operators, $\kappa_{qk,q'k'}$ and $\eta_{qk,q'k'}$ are the corresponding strength matrices. We need these two kinds of the operators since the relevant Skyrme functionals involve both time-even and time-odd densities, see [1, 26, 30, 31, 32].

The starting point is a Skyrme functional $E[J_q^\alpha(\mathbf{r},t)] = \int d\mathbf{r}\mathcal{H}_{\rm Sk}(\mathbf{r},t)$, say that in (1), with a set of local densities J_q^α. The separable operators and strength matrices are derived from the functional by using the scaling transformation for the perturbed wave function of the system:

$$|\Psi(t)\rangle_q = \prod_{k=1}^{K}\exp[-i\varrho_{qk}(t)\hat{P}_{qk}]\exp[-ip_{qk}(t)\hat{Q}_{qk}]|\rangle_q \tag{A2}$$

were both $|\Psi(t)\rangle_q$ and ground state $|\rangle_q$ are Slater determinants, $\hat{Q}_{qk}(\mathbf{r})$ and $\hat{P}_{qk}(\mathbf{r})$ are generalized coordinate (time-even) and momentum (time-odd) hermitian one-body input operators, $\hat{H}$ stands for the full Hamiltonian. For Eλ modes, the input operators $\hat{Q}_{qk}(\mathbf{r})$ determine $\hat{P}_{qk}(\mathbf{r}) = i[\hat{H},\hat{Q}_{qk}]$, while for M$\lambda$ modes, the input operators $\hat{P}_{qk}(\mathbf{r})$ gives $\hat{Q}_{qk}(\mathbf{r}) = i[\hat{H},\hat{P}_{qk}]$. Further

$$\varrho_{qk}(t) = \bar{\varrho}_{qk}\cos(\omega t)\ , p_{qk}(t) = \bar{p}_{qk}\sin(\omega t) \tag{A3}$$

are corresponding collective variables. As seen from (A2), the input operators are determined up to arbitrary constant multipliers whose action can be compensated by the proper rescaling the collective variables.

The number K of input operators in (A2) determines the number of the separable terms in $\hat{V}_{\rm res}^{\rm sep}$. The treatment converges to exact RPA for $K \to \infty$. In practice, a good approximation to RPA is already obtained for a small $K = 2 \div 5$ if the input operators $\hat{Q}_{qk}$ ($\hat{P}_{qk}$) are properly chosen.

The separable operators and (inverse) strength matri-

ces in (A1) are self-consistently constructed as [26, 30, 31]

$$\hat{X}_{qk} = \sum_{q'} \hat{X}^{q'}_{qk} = i \sum_{\alpha' \alpha q'} \frac{\delta^2 E}{\delta J^{\alpha'}_{q'} \delta J^{\alpha}_{q}} \langle [\hat{P}_{qk}, \hat{J}^{\alpha}_{q}] \rangle \hat{J}^{\alpha'}_{q'} , \quad \text{(A4)}$$

$$\hat{Y}_{qk} = \sum_{q'} \hat{Y}^{q'}_{qk} = i \sum_{\alpha' \alpha q'} \frac{\delta^2 E}{\delta J^{\alpha'}_{q'} \delta J^{\alpha}_{q}} \langle [\hat{Q}_{qk}, \hat{J}^{\alpha}_{q}] \rangle \hat{J}^{\alpha'}_{q'} , \quad \text{(A5)}$$

$$\kappa^{-1}_{q'k',qk} = \sum_{\alpha \alpha'} \frac{\delta^2 E}{\delta J^{\alpha'}_{q'} \delta J^{\alpha}_{q}} \langle [\hat{P}_{qk}, \hat{J}^{\alpha}_{q}] \rangle \langle [\hat{P}_{q'k'}, \hat{J}^{\alpha'}_{q'}] \rangle , \quad \text{(A6)}$$

$$\eta^{-1}_{q'k',qk} = \sum_{\alpha \alpha'} \frac{\delta^2 E}{\delta J^{\alpha'}_{q'} \delta J^{\alpha}_{q}} \langle [\hat{Q}_{qk}, \hat{J}^{\alpha}_{q}] \rangle \langle [\hat{Q}_{q'k'}, \hat{J}^{\alpha'}_{q'}] \rangle \quad \text{(A7)}$$

where $\hat{J}^{\alpha}_{q}$ are the density operators.

The final RPA equations have the form

$$\sum_{qk} \{ \bar{\varrho}^{\nu}_{qk} [F^{(XX)}_{q'k',qk} - \kappa^{-1}_{q'k',qk}] + \bar{p}^{\nu}_{qk} F^{(XY)}_{q'k',qk} \} = 0, \quad \text{(A8)}$$

$$\sum_{qk} \{ \bar{\varrho}^{\nu}_{qk} F^{(YX)}_{q'k',sk} + \bar{p}^{\nu}_{qk} [F^{(YY)}_{q'k',qk} - \eta^{-1}_{q'k',qk}] \} = 0 \quad \text{(A9)}$$

with

$$F^{(AB)}_{q'k',qk} = 2 \sum_{q",ph \in q"} \alpha_{AB} \frac{\langle ph | \hat{A}^{q"}_{qk} | \rangle^* \langle ph | \hat{B}^{q"}_{q'k'} | \rangle}{\varepsilon^2_{ph} - \omega^2_{\nu}} \quad \text{(A10)}$$

and

$$\alpha_{AB} = \begin{pmatrix} \varepsilon_{ph}, & \text{for } \hat{A} = \hat{B} \\ -i\omega_{\nu}, & \text{for } \hat{A} = \hat{Y}, \hat{B} = \hat{X} \\ i\omega_{\nu}, & \text{for } \hat{A} = \hat{X}, \hat{B} = \hat{Y} \end{pmatrix} . \quad \text{(A11)}$$

Here $\langle ph | \hat{A}^{q"}_{q'k'} | \rangle$ is the matrix element for the two-quasiparticle state $|ph\rangle$, ε_{ph} is the energy of this state, ω_{ν} is the energy of the RPA state $|\nu\rangle$. The amplitudes of the RPA phonon operator

$$\hat{C}^{\dagger}_{\nu} = \sum_{q} \sum_{ph \in q} \left(c^{\nu -}_{ph} \hat{A}^{\dagger}_{ph} - c^{\nu +}_{ph} \hat{A}_{ph} \right) \quad \text{(A12)}$$

are determined via solutions of (A8)-(A9)

$$c^{\nu \pm}_{ph \in q} = - \sum_{q'k'} \frac{\bar{\varrho}^{\nu}_{q'k'} \langle ph | \hat{X}^{q}_{q'k'} \rangle \mp i \bar{p}^{\nu}_{q'k'} \langle ph | \hat{Y}^{q}_{q'k'} \rangle}{2(\varepsilon_{ph} \pm \omega_{\nu})} \quad \text{(A13)}$$

and $\hat{A}^{\dagger}_{ph}$ and $\hat{A}_{ph}$ are operators of creation and destruction of two-quasiparticle states.

Following (A4)-(A7), the separable ansatz (A1) explores the residual interaction of the Skyrme functional through the second functional derivatives. The calculations show that for spin-flip magnetic modes the spin

$$\frac{\delta^2 E}{\delta \mathbf{s}_{q'}(\mathbf{r}') \delta \mathbf{s}_{q}(\mathbf{r})} = \Big[\tilde{b}_0 - \tilde{b}'_0 \delta_{qq'} + \tilde{b}_3 \frac{2}{3} \rho^{\alpha}(\mathbf{r}) - \frac{2}{3} \tilde{b}'_3 \rho^{\alpha}(\mathbf{r}) \delta_{qq'} - (\tilde{b}_2 - \tilde{b}'_2 \delta_{qq'}) \Delta_{\mathbf{r}} \Big] \delta(\mathbf{r} - \mathbf{r}') , \quad \text{(A14)}$$

spin-orbit

$$\frac{\delta^2 E}{\delta \mathbf{J}_{q'}(\mathbf{r}') \delta \rho_{q}(\mathbf{r})} = (b_4 + b'_4 \delta_{qq'}) \nabla_{\mathbf{r}} \delta(\mathbf{r} - \mathbf{r}') , \quad \text{(A15)}$$

$$\frac{\delta^2 E}{\delta \mathbf{j}_{k;q'}(\mathbf{r}') \delta \mathbf{s}_{l;q}(\mathbf{r})} = (b_4 + b'_4 \delta_{qq'}) (\varepsilon_{klm} \nabla_{m;\mathbf{r}}) \delta(\mathbf{r} - \mathbf{r}') ,$$

and tensor terms

$$\frac{\delta^2 E}{\delta \mathbf{J}_{q'}(\mathbf{r}') \delta \mathbf{J}_{q}(\mathbf{r})} = -2(\tilde{b}_1 + \tilde{b}'_1 \delta_{qq'}) \delta(\mathbf{r} - \mathbf{r}') , \quad \text{(A16)}$$

$$\frac{\delta^2 E}{\delta \mathbf{T}_{q'}(\mathbf{r}') \delta \mathbf{s}_{q}(\mathbf{r})} = (\tilde{b}_1 + \tilde{b}'_1 \delta_{qq'}) \delta(\mathbf{r} - \mathbf{r}') \quad \text{(A17)}$$

are most important.

SRPA equations presented above are obtained for arbitrary functionals $E[J^{\alpha}_{q}(\mathbf{r}, t)]$, including Skyrme ones. The model is self-consistent in the sense that both the static mean field

$$\hat{h}_0 = \sum_{\alpha q} \frac{\delta E}{\delta J^{\alpha}_{q}} \hat{J}^{\alpha}_{q} \quad \text{(A18)}$$

and the residual interaction (A1), (A4)-(A7) are derived from the same functional. The rank of the RPA matrix (A8)-(A9) is determined by the number K of the input operators in (A2). As was mentioned above, usually $K = 2 \div 5$ and so the rank is very small [26, 27, 28, 29]. This drastically simplifies RPA computational effort and allows to perform systematic explorations even for heavy deformed nuclei.

APPENDIX B: SRPA STRENGTH FUNCTION

Giant resonances in heavy nuclei are formed by many RPA states whose detailed contributions cannot be resolved experimentally. Then, instead of solution of Eqs. (A8)-(A9), a direct computation of the strength function (4) is more efficient and reasonable. In SRPA it reads

$$S(M1; \omega) = \sum_{\nu \neq 0} |\langle \Psi_{\nu} | \hat{M} | \Psi_0 \rangle|^2 \zeta(\omega - \omega_{\nu}) \quad \text{(B1)}$$

$$= \Im \left[\frac{z^L \sum_{\beta \beta'} F_{\beta \beta'}(z) D_{\beta}(z) D_{\beta'}(z)}{\pi F(z)} \right]_{z = \omega + i\Delta/2} + \sum_{q} \sum_{ph \in q} \varepsilon_{ph} \langle ph | \hat{M} | \rangle^2 \zeta(\omega - \varepsilon_{ph})$$

where $\beta = qk\tau$ with τ being the time parity, $\Im$ means the imaginary part of the value inside the brackets, $F(z)$ is the determinant of the RPA matrix (A8)-(A9) with ω_{ν} replaced by the complex argument z, $F_{\beta\beta'}(z)$ is the algebraic supplement of the determinant, and

$$D^{(X)}_{qk}(z) = \sum_{q'} \sum_{ph \in q'} \frac{\omega_{\nu} \langle ph | X^{q'}_{qk} | \rangle \langle ph | \hat{M} | \rangle}{\varepsilon^2_{ph} - z^2} , \quad \text{(B2a)}$$

$$D^{(Y)}_{qk}(z) = i\sum_{q'}\sum_{ph\in q'}\frac{\varepsilon_{ph}\langle ph|Y^{q'}_{qk}|\rangle\langle ph|\hat{M}|\rangle}{\varepsilon^2_{ph}-z^2}\ . \qquad \text{(B2b)}$$

In the present study we are interested only in spin-flip M1 mode. So the strength function is calculated only for $\mu = 1$ branch of magnetic dipole excitations. The branch with $\mu = 0$ is omitted as it does not support pure spin-flip transitions but only its mixture with orbital modes.

APPENDIX C: INPUT OPERATORS

The SRPA formalism itself does not provide the input operators $\hat{P}_{qk}(\mathbf{r})$ in the scaling transformation (A2). At the same time, their choice is crucial to converge the approximate residual interaction $\hat{V}^{\rm sep}_{\rm res}$ to the true Skyrme one with a minimal number of the separable terms. We achieve this aim by using $\hat{P}_{qk}(\mathbf{r})$-inputs which compel the separable operators $\hat{X}_{qk}(\mathbf{r})$ and $\hat{Y}_{qk}(\mathbf{r})$ to have maxima in different spatial regions of the nucleus, both in the surface and interior. The analysis shows that this way indeed allows to get good convergence already with a few separable terms.

The physical arguments suggest that the leading scaling operator $\hat{P}_{q1}(\mathbf{r})$ should have the form of the applied external field in the long-wave approximation, in our case of magnetic field of multipolarity $\lambda\mu = 11$. In present calculations we take decoupled spin and orbital input operators $\hat{P}_{q1} = \hat{s}^q_+$ and $\hat{P}_{q2} = \hat{l}^q_+$ and supplement them by $\hat{P}_{q3} = r^2\hat{s}^q_+$ and $\hat{P}_{q4} = r^2\hat{l}^q_+$. Then altogether we have K=4 input operators and the corresponding operators $\hat{X}_{qk}(\mathbf{r})$ and $\hat{Y}_{qk}(\mathbf{r})$ have maxima in both surface and interior of the nucleus.

In deformed nuclei we should take into account the coupling between magnetic and electric $K^\pi = 1^+$ states. So the quadrupole input operator $Q_{q5} = r^2Y_{21}(\Theta)$ with the counterpart $\hat{P}_{q5} = i[\hat{H}, \hat{Q}_{q5}]$ is added. Then K=5 and we have the RPA matrix of the rank 4K=20.

In terms of two-quasiparticle matrix elements, the relations between input operators are reduced to

$$\begin{aligned}\hat{Q}_{qk}(\mathbf{r}) &= i[\hat{H}, \hat{P}_{qk}] \rightarrow \\ \langle ph|\hat{Q}_{qk}|0\rangle &= 2\varepsilon_{ph}\langle ph|\hat{P}_{qk}|0\rangle - \langle ph|\hat{X}^q_{qk}|0\rangle \qquad \text{(C1)}\end{aligned}$$

for magnetic modes and

$$\begin{aligned}\hat{P}_{qk}(\mathbf{r}) &= i[\hat{H}, \hat{Q}_{qk}] \rightarrow \\ \langle ph|\hat{P}_{qk}|0\rangle &= 2\varepsilon_{ph}\langle ph|\hat{Q}_{qk}|0\rangle - \langle ph|\hat{Y}^q_{qk}|0\rangle \qquad \text{(C2)}\end{aligned}$$

for electric modes.

For more details see [26, 30, 31, 32].

[1] M. Bender, P.-H. Heenen, and P.-G. Reinhard, Rev. Mod. Phys. **75**, 121 (2003).
[2] D. Vretenar, A.V. Afanasjev, G.A. Lalazissis, and P. Ring, Phys. Rep. **409**, 101 (2005).
[3] J. R. Stone and P.-G. Reinhard, Prog. Part. Nucl. Phys. **58**, 587 (2007).
[4] P.-G. Reinhard, Nucl. Phys. **A649**, 305c (1999).
[5] P. Klüpfel, P.-G. Reinhard, T. J. Bürvenich, J. A. Maruhn, Phys. Rev. C **79**, 034310 (2009).
[6] T. Lesinski, M. Bender, K. Bennaceur, T. Duguet, and J. Meyer, Phys. Rev. C **76**, 141312 (2007).
[7] M. Bender, J. Dobaczewski, J. Engel, and W. Nazarewicz, Phys. Rev. C **65**, 054322 (2002).
[8] S. Fracasso and G. Colo, Phys. Rev. C **76**, 144307 (2007).
[9] P. Sarriguren, E. Moya de Guerra, and A. Escuderos, Nucl. Phys. **A69**, 631 (2001).
[10] Int. Rew. Nucl. Phys. **7**, ed. J. Speth (World Sientific, Singapore, 1991).
[11] F. Osterfeld, Rev. Mod. Phys. **64**, 491 (1992).
[12] M.N. Harakeh and A. van der Woude, *Giant Resonances* (Clarendon Press, Oxford, 2001).
[13] P. Sarriguren, E. Moya de Guerra, and R. Nojarov, Phys. Rev. C **54**, 690 (1996).
[14] R.R. Hilton, W. Höbenberger, and P. Ring, Eur. Phys. J. A**1**, 257 (1998).
[15] H.L. Wörtche, Ph.D. thesis, Technischen Hochschule Darmstadt, Germany, 1994.
[16] D. Frekers et al, Phys. Lett. B**244**, 178 (1990).
[17] S. K. Nanda et al, Phys. Rev. C **29**, 660 (1984); A. Richter, Phys. Scripta, T**5**, 63 (1983).
[18] R. M. Laszewski, R. Alarcon, D. S. Dale, S. D. Hoblit, Phys. Rev. Let. **61**, 1710 (1988).
[19] T. Shizuma et al, Phys. Rev. C **78**, 061303 (2008).
[20] F. Tondeur, M. Brack, M. Farine, and J.M. Pearson, Nucl. Phys. **A420**, 297 (1984).
[21] P.-G. Reinhard, D.J. Dean, W. Nazarewicz, J. Dobaczewski, J.A. Maruhn, and M.R. Strayer, Phys. Rev. C **60**, 14316 (1999).
[22] N. Van Giai and H. Sagawa, Phys. Lett. B **106**, 379 (1981).
[23] J. Bartel, P. Quentin, M. Brack, C. Guet, and H.-B. Håakansson, Nucl. Phys. **A386**, 79 (1982).
[24] E. Chabanat, P. Bonche, P. Haensel, J. Meyer, and R. Schaeffer, Nucl. Phys. **A627**, 710 (1997).
[25] P.-G. Reinhard and H. Flocard, Nucl. Phys. **A584**, 467 (1995).
[26] V.O. Nesterenko, W. Kleinig, J. Kvasil, P. Vesely, P.-G. Reinhard, and D.S. Dolci, Phys. Rev. C **74**, 064306 (2006).
[27] V.O. Nesterenko, W. Kleinig, J. Kvasil, P. Vesely, and P.-G. Reinhard, Int. J. Mod. Phys. E **16**, 624 (2007).
[28] V.O. Nesterenko, W. Kleinig, J. Kvasil, P. Vesely, and P.-G. Reinhard, Int. J. Mod. Phys. E **17**, 89, (2008).
[29] W. Kleinig, V.O. Nesterenko, J. Kvasil, P.-G. Reinhard, and P. Vesely, Phys. Rev. C **78**, 044313 (2008).
[30] V.O. Nesterenko, J. Kvasil, and P.-G. Reinhard, Phys. Rev. C **66**, 044307 (2002).
[31] V.O. Nesterenko, J. Kvasil, W. Kleinig, P.-G. Reinhard, and D.S. Dolci, arXiv: nucl-th/0512045.
[32] P. Vesely, Ph. D. thesis, Charles University in Prague,

Czech Rep., 2009.